Ultra-flat bands in two-dimensional photonic crystals

Mihai Ibanescu[a], Marin Soljacic[a], Steven G. Johnson[b], and J. D. Joannopoulos[a]

[a] Department of Physics, Massachusetts Institute of Technology, Cambridge, MA 02139, USA
[b] Department of Mathematics, Massachusetts Institute of Technology, Cambridge, MA 02139, USA

ABSTRACT

We show that two-dimensional photonic crystals can be designed to have dispersion relations with an extended ultra-flat cross-section, meaning that for a fixed wave vector component k_x the frequency of a band is almost constant when the other wave vector component, k_y, takes all possible values. These ultra-flat bands are the result of a non-trivial saddle point in the dispersion relation located in the interior of the Brillouin zone. Interesting consequences include 1D-like behavior, improved super-collimation, and enhanced density of states.

Keywords: photonic crystal, ultra-flat band, saddle point

1. INTRODUCTION

Flat regions in the band structures of photonic crystals have been studied due to their role in achieving or enhancing a variety of optical effects, including enhancement of the photonic density of states, lasing, super-collimation, enhanced nonlinear effects, and other slow-light effects [1–4]. The flat parts of dispersion relations and the associated reduced group velocities are generally found in limited regions around symmetry points in wave vector space . However, as the dimensionality of the photonic crystal increases from 1-d to 2-d and 3-d, these flat regions around symmetry points tend to occupy a decreasing fraction of the entire volume of the Brillouin zone. Furthermore, the band structures of two-dimensional and three-dimensional photonic crystals are in general more complex than those of one-dimensional crystals for the obvious reason that the frequency of a mode is a function of two or three wave vector components, instead of just one. Here, we find that a two-dimensional square photonic crystal can be designed to have an *extended* ultra-flat cross-section of the dispersion relation $\omega(k_x, k_y)$, meaning that, for a fixed k_x, the frequency range of $\omega(k_y)$ can be extremely narrow when k_y takes *all* possible values in the Brillouin zone. These extended ultra-flat bands are the result of a non-trivial saddle point that is not located at a symmetry point, but rather in the interior of the Brillouin zone.

2. RESULTS

Consider the two-dimensional square lattice of dielectric rods depicted in Fig. 1(a). The rods have an index of refraction $n = 3.4$ and a radius $r = 0.13a$, where a is the lattice period. We calculate the band structure of this crystal with a frequency-domain plane-wave expansion method [5]. The dispersion relations $\omega(k_x, k_y)$ of the lowest two transverse-magnetic (TM) modes are plotted in Fig. 1(b). The black lines represent $\omega(k_x)$ curves at fixed k_y values ranging from $k_y = 0$ to $k_y = 0.5$ (all wave vectors are in units of $2\pi/a$). The surprising feature of the band structure is the presence of a very narrow cross-section in the middle second band, indicated by the thick black arrow. For $k_x = 0.252$, the angular frequency ω of this band varies by only 1.6% when k_y goes from one end of the Brillouin zone to another.

In Fig. 1(c) we plot the entire dispersion relation for the second band as a contour plot. We find that the ultra-flat region of the dispersion relation at $k_x = 0.252$ is the result of a saddle point in $\omega(k_x, k_y)$ located at $k_x = k_y = 0.24$ and displayed as a black dot in the figure. Around the saddle point the curvature of the band as a function of direction has a positive maximum and a negative minimum corresponding to the two principal axes of the saddle point. Since the $k_x = const.$ direction is at a 45 degree angle with respected to the principal axes, we find a very small curvature

Photonic Crystal Materials and Devices IV, edited by Ali Adibi, Shawn-Yu Lin, Axel Scherer,
Proc. of SPIE Vol. 6128, 612808, (2006) · 0277-786X/06/$15 · doi: 10.1117/12.652776

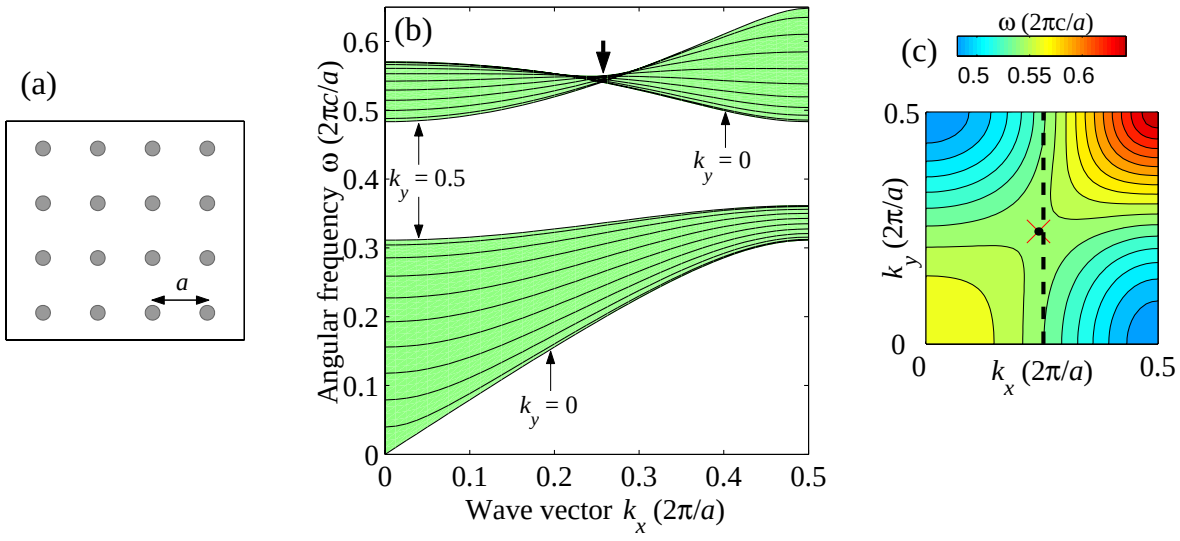

Figure 1. (a) Square lattice of rods with index of refraction $n = 3.4$ and radius $r = 0.134a$. (b) Projected TM band structure of the photonic crystal in (a). The black lines represent $\omega(k_x)$ curves at fixed k_y values ranging from $k_y = 0$ to $k_y = 0.5\,(2\pi/a)$ in steps of $0.05\,(2\pi/a)$. The thick arrow indicates an ultra-flat cross-section of the second band. (c) Contour plot of the second band $\omega(k_x, k_y)$. The saddle point and its principal axes are indicated by the black dot and two red lines. The extended ultra-flat band is along the dashed line.

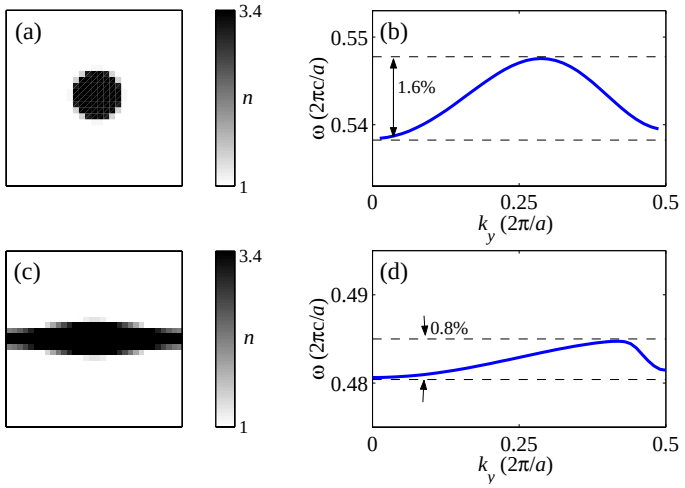

Figure 2. (a) Index of refraction $n(x, y)$ in the unit cell for the structure in Fig. 1(a). For band calculations, the unit cell has been discretized over a 30x30 grid. (b) Ultra-flat dispersion relation $\omega(k_y)$ at $k_x = 0.252$ for the photonic crystal in part (a). (c) Improved structure, with $\max(n) = 3.4$. (d) For the structure in part (c), at $k_x = 0.006$, the $\omega(k_y)$ band has a width of only 0.8%.

of the band in this direction. This fact together with the requirement that the group velocity of a photonic band is zero at the Brillouin zone edge results in the ultra-flat band. Fig. 2(b) shows the actual dispersion relation $\omega(k_y)$ of the ultra-flat band. The range of frequencies found in the bend is of only 1.6% and the group velocity throughout the bend is less than $0.05c$ in absolute value.

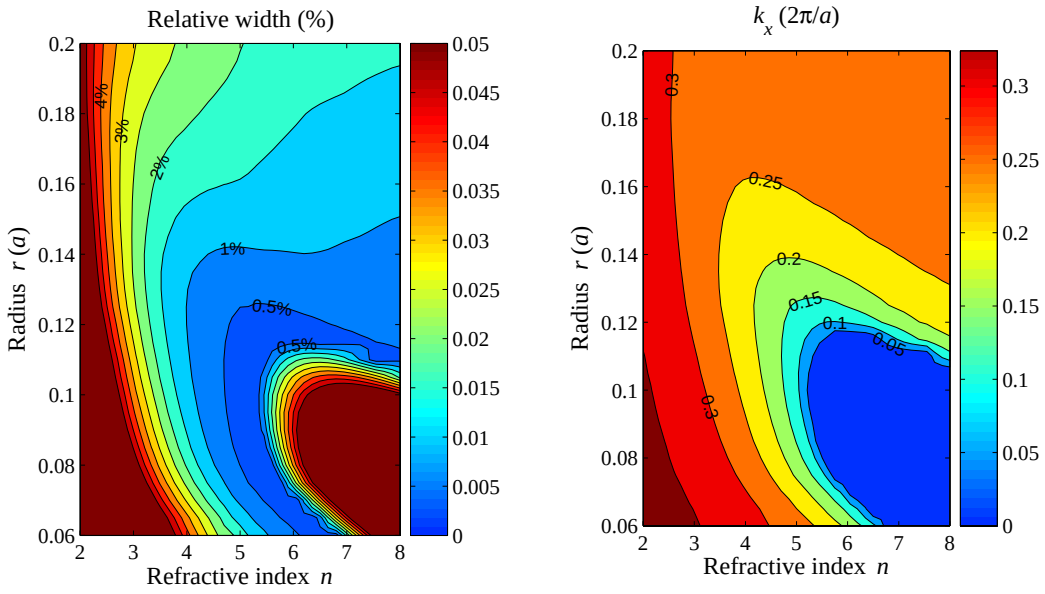

Figure 3. (a) For each pair of refractive index n and rod radius r the minimum achievable relative width $w(n, r)$ of the band is plotted as a color contour plot. The color scheme is such that the width decreases from red to green to blue. Contour levels are shown only for widths less than 5%. (b) Contour plot of the wave vector k_x at which the minimum width was found for each pair $(n,\ r)$. In the lower right corner k_x is zero or very close to zero.

The minimum width of 1.6% was obtained by optimizing for the rod radius r, but assuming the dielectric distribution is a circle. Even narrower widths can be achieved if we allow for other distributions of the index of refraction $n(x, y)$ in the unit cell. Such an improved structure is shown in Fig. 2(c). A width of only 0.8% is now found for the $\omega(k_y)$ band in Fig. 2(d). The y-direction group velocity in most of the band is below $0.01c$. The improved dielectric distribution was obtained by writing $n(x, y)$ as a sum of several sinusoidal functions in x and y and optimizing with respect to the coefficients of these functions. A structure with $max(n) = 3.4$ that results in an even smaller width is likely to exist.

A large index of refraction n is desirable for obtaining extended ultra-flat bands. This trend is illustrated in Fig. 3(a) where for each pair of refractive index n and rod radius r the minimum achievable relative width $w(n, r)$ of the band is plotted as a color contour plot. In Fig. 3(b) we plot the wave vector k_x for which this minimum width was achieved. We notice that, in most cases, an increased index of refraction results in a smaller width.

An interesting trend can be observed also if we look at the optimum radius r of dielectric rod. For several values of n we find the rod radius r that results in a band with the smallest width, and we compile the results in Table 1. The minimum achievable width decreases significantly when n is increased, the dependence being roughly exponential in this range of parameters.

Table 1. Variation of the minimum band width with index of refraction n

n	2.80	3.40	4.00	4.60	5.20
r/a	0.156	0.134	0.119	0.109	0.110
Minimum width $w = \Delta\omega/\omega$	2.9%	1.6%	0.94%	0.46%	0.22%

Next, we explore in more detail the relationship between the ultra-flat band and the presence of saddle point in the

interior of the Brillouin zone. We start with the folded band structure of vacuum shown in Fig. 4(a). In this case the second band is clearly divided into two regions, one below and one above the ΓM line. Both regions have circular equi-frequency contours, but one originates from band folding in the x direction and the other in the y direction. In Fig 4(b) we see that the introduction of a dielectric perturbation (a dielectric rod with radius $r = 0.06a$) results in a saddle point located along the ΓM line, shown as a black dot in the figure. In fact, this saddle point is present for other dielectric perturbations as well and is due to a mirror symmetry that exists at M but is broken as we move away from this symmetry point [6]. The minimum width of $k_x = const.$ cross-sections is found around $k_x = 0.34\,(2\pi/a)$ and is less than 8%. Increasing the radius of dielectric rods to $r = 0.12a$ (Fig 4(c)) moves the saddle point closer to the midway point between Γ and M and results in a much lower minimum width (1.6% at $k_x = 0.26\,(2\pi/a)$). Figure 4(d) shows in a more quantitative manner how the frequencies of the second band are modified by the introduction of the dielectric rods. We plot the difference between $\omega(k_x, k_y)$ for the vacuum case ($r = 0$) and for $r = 0.06a$. We see that along the $k_x = 0.26$ line the frequency change is very small around $k_y = 0.5$ and is maximum (in absolute value) around $k_y = 0.25$.

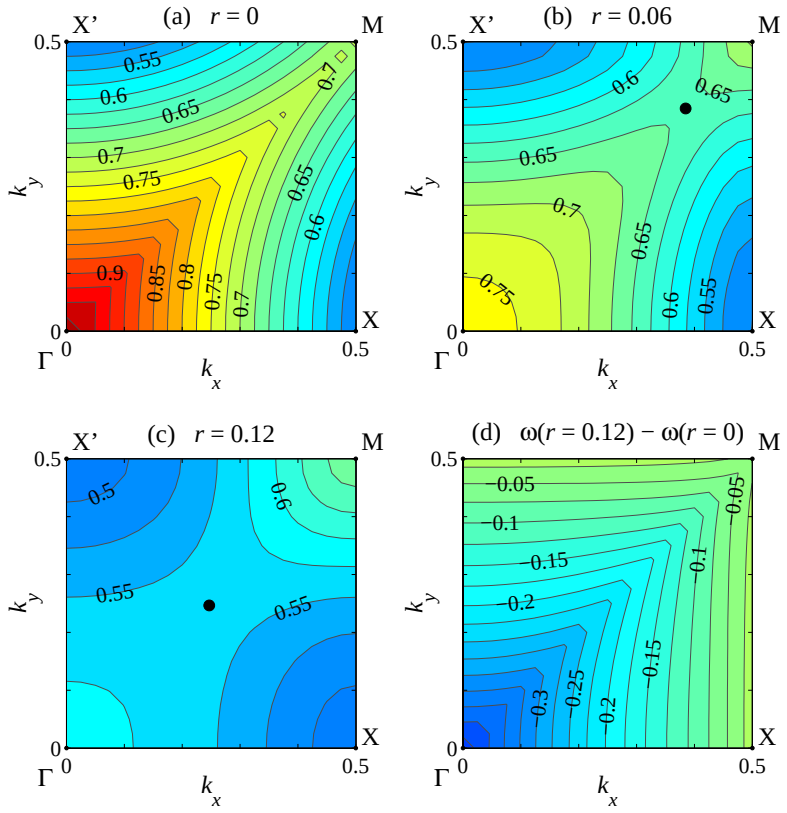

Figure 4. (a) Contour plot for the second band $\omega(k_x, k_y)$ for the photonic crystal when the radius r of the rods is taken to 0 (folded band structure of vacuum). The equi-frequency contours are circular on both sides of the ΓM line. (b) For a rod radius $r = 0.06a$ the band develops a saddle point near the M point. (c) For $r = 0.12a$ the saddle point moves to approximately half-way between Γ and M and creates an ultra-flat region of the band. (d) The change in the frequency of the second band between the vacuum case (part (a)) and the $r = 0.12a$ case (part (c)).

To understand the variation of the frequency change mentioned above, in Fig. 5 we look at the distribution of the electric field throughout the unit cell at $k_x = 0.26$ and $k_y = 0$, 0.25, and 0.5. From perturbation theory we can expect a larger frequency change when there is a larger amplitude of the electric field inside the dielectric rods. The first thing

to notice is that at $k_y = 0.5$ the dielectric rods are always in the nodes of the electric field distribution, which means that the frequency should be almost insensitive to the introduction of the dielectric rods. This is indeed confirmed by Fig 4(d) .

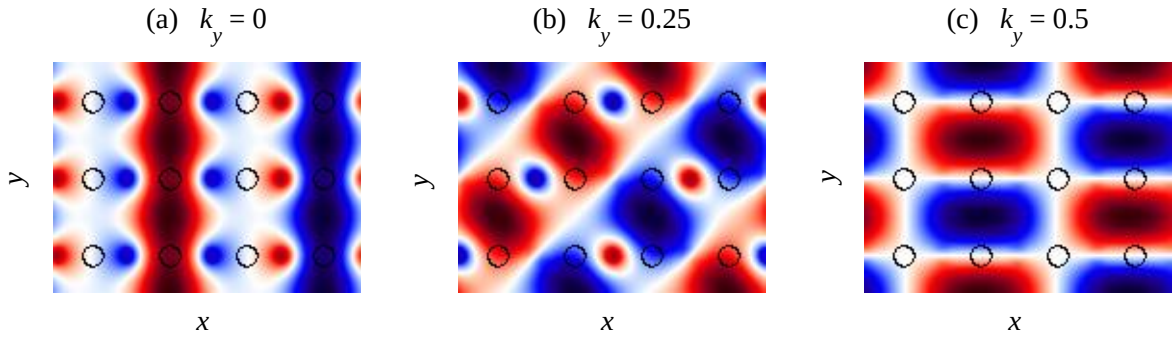

Figure 5. Spatial distribution of E_z, the z-component of the electric field, along the ultra-flat band at (a) $k_y = 0$, (b) $k_y = 0.25\,(2\pi/a)$, and (c) $k_y = 0.5\,(2\pi/a)$. For all three cases k_x is $0.26\,(2\pi/a)$. The black circles are the outlines of the dielectric rods.

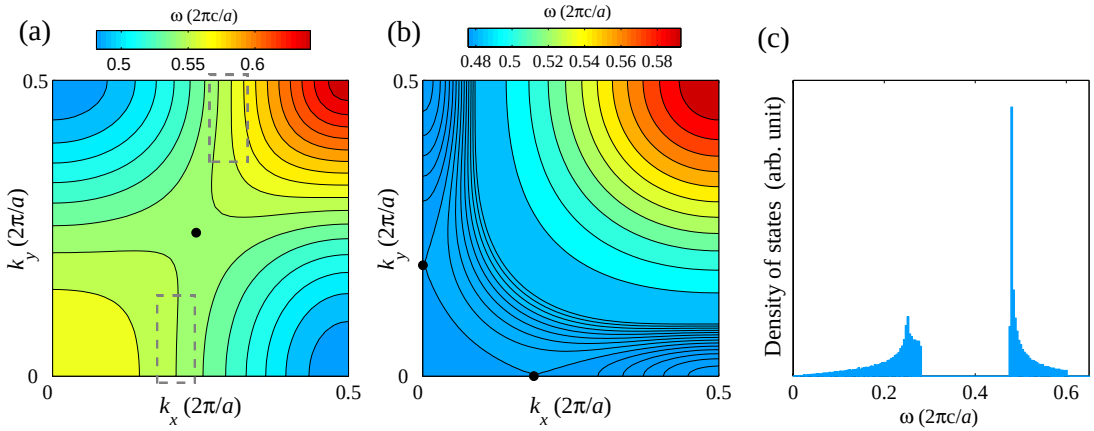

Figure 6. (a) Contour plot of $\omega(k_x, k_y)$ for the structure of Fig. 1(a). Two self-collimation are outlined by dotted rectangular boxes. (b) Ultra-flat band for rods with $n = 5.2$ and $r = 0.11a$. The saddle point has now moved to the x and y axes. For $k_x = 0.05$, $\omega(k_y)$ has a relative bandwidth of only 0.25%. Note that the lowest ten contour levels in the bottom-left part of graph are separated by only $5\text{x}10^{-4}\,(2\pi c/a)$ in frequency. (c) The density of states associated with the photonic band in part (b) presents a strong logarithmic divergence at $\omega = 0.48$ due to the ultra-flat region around the saddle point.

We now discuss potential applications of extended ultra-flat bands. The super-collimation effect in photonic crystals is made possible by flat equi-frequency contours in the (k_x, k_y) plane [2]. Fig. 6(a) outlines two regions in reciprocal space where super-collimation would occur for the case of the photonic crystal in Fig. 1(a). Even more interestingly, in the limit of a perfectly flat band ($\omega(k_y) = \omega_0$ at fixed k_x), the two self-collimation regions would merge and create a line of perfect collimation: light of frequency ω_0 would travel in the x-direction irrespective of the transverse wave vector k_y, allowing for non-dispersing beams with a beam width as small as one unit cell! In this limit, the two-dimensional crystal would have a quasi-1D behavior at $\omega = \omega_0$.

In Fig. 6(b) we show that, for a lattice of rods with index of refraction $n = 5.2$ and radius $r = 0.11a$, the non-

trivial saddle point gives rise to an ultra-flat band (relative width 0.2%) along the $k_x = 0$ line, and also to a reduced group-velocity region throughout the bottom part and the left part of the Brillouin zone. This results in a logarithmic divergence with a large prefactor in the density of states around $\omega = 0.48$, as seen in Fig. 6(c).

3. CONCLUSIONS

We have shown that two-dimensional square photonic crystals can be designed to have extended ultra-flat bands along certain lines in wave vector space. After creating bands with relative width as low as 0.1% in some structures, we plan to pursue the theoretical challenge of whether or not it is possible to obtain a perfectly flat band, one with $\omega(k_y) = $ const. at fixed k_x. Even though we presented results only for TM modes in 2D photonic crystals, similar effects occur with TE modes, and we believe the effects should apply to the band structures of photonic crystal slabs as well.

REFERENCES

1. A. Mekis, M. Meier, A. Dodabalapur, R. E. Slusher, and J. D. Joannopoulos, "Lasing mechanism in two-dimensional photonic crystal lasers," *Appl. Phys. A* **69**, pp. 111–114, 1999.
2. H. Kosaka, T. Kawashima, A. Tomita, M. Notomi, T. Tamamura, T. Sato, and S. Kawakami, "Self-collimating phenomena in photonic crystals," *Appl. Phys. Lett.* **74**, pp. 1212–1214, 1999.
3. M. Soljacic, S. G. Johnson, S. Fan, M. Ibanescu, E. Ippen, and J. D. Joannopoulos, "Photonic-crystal slow-light enhancement of nonlinear phase sensitivity," *J. Opt. Soc. Am. B* **19**, pp. 2052–2059, 2002.
4. M. F. Yanik and S. Fan, "Stopping light all optically," *Phys. Rev. Lett.* **92**, p. 083901, 2004.
5. S. G. Johnson and J. D. Joannopoulos, "Block-iterative frequency-domain methods for Maxwell's equations in a planewave basis," *Opt. Express* **8**(3), pp. 173–190, 2001.
6. M. Ibanescu, E. J. Reed, and J. D. Joannopoulos, "Enhanced band-gap confinement via van hove saddle point singularities," *Phys. Rev. Lett.* , 2006. (in press).